chemistry

MDPI

Communication

Solid-State ^{2}H NMR Study for Deuterated Phenylene Dynamics in a Crystalline Gyroscope-Like Molecule

Wataru Setaka [1,*], Kentaro Yamaguchi [2] and Mitsuo Kira [3]

[1] Division of Applied Chemistry, Faculty of Urban Environmental Sciences, Tokyo Metropolitan University, 1-1 Minami-Osawa, Hachioji, Tokyo 192-0397, Japan
[2] Faculty of Pharmaceutical Sciences at Kagawa Campus, Tokushima Bunri University, 1314-1 Shido, Sanuki, Kagawa 769-2193, Japan; kyamaguchi@kph.bunri-u.ac.jp
[3] Key Laboratory of Organosilicon and Material Technology of Education Ministry, Hangzhou Normal University, Hangzhou 311121, China; mitsuo.kira.e2@tohoku.ac.jp
* Correspondence: wsetaka@tmu.ac.jp; Tel.: +81-42-677-1111

Abstract: Molecular rotors have earned substantial popularity in recent times, owing to the unique dependence of its crystalline properties on the rotational dynamics of the rotor. We have recently reported the synthesis and crystal structure of a phenylene-bridged macrocage as a gyroscope-like molecule in the crystalline state. The dynamics of the phenylene moiety was probed by solid-state ^{13}C CP/MAS proton dipolar dephasing NMR spectroscopy. Herein, solid-state ^{2}H NMR studies were performed to study the dynamics of the gyroscope-like molecule with a deuterated rotor in the crystalline state. A spectrum with a narrow line shape was obtained at 300 K. The facile exchange among three stationary states, which was observed by X-ray crystallography, was clearly confirmed. Additionally, a crystal-to-crystal phase transition that switches the motion of the rotor was observed in the DSC analysis of the powdered sample.

Keywords: crystalline molecular rotor; solid-state ^{2}H NMR; artificial molecular machine

Citation: Setaka, W.; Yamaguchi, K.; Kira, M. Solid-State ^{2}H NMR Study for Deuterated Phenylene Dynamics in a Crystalline Gyroscope-Like Molecule. *Chemistry* **2021**, *3*, 39–44. https://doi.org/10.3390/chemistry3010004

Received: 13 December 2020
Accepted: 5 January 2021
Published: 7 January 2021

1. Introduction

Molecular rotors, in which a part of the molecule rotates, even in the crystalline state, have recently attracted considerable attention in the field of molecular machines [1–3]. In the last few years, many molecular rotors have been reported and their properties studied in depth. Molecular rotors with functional anchors have been reported by Kaleta and Michl [4], while rotors with bulky stators have been studied by Garcia-Garibay, as well as other researchers [5]. Molecular rotors that are encased by a cage have been reported by Gladysz [6], Garcia-Garibay [7], and our group [8–15]. Particularly, we have focused on the properties of the crystal modulated by the dynamics of the molecule. We have recently reported changes in the birefringence of a crystal as a function of temperature, arising from the switch between the static and dynamic states of the molecular rotor [8,9]. We have also studied the inflation of a phenylene bridged macrocage crystal that was caused due to the rotation of the rotor in it [10]. The dielectric relaxation of a powdered molecular dipolar rotor [11] has been reported by our group as well.

We have previously reported the synthesis and crystal structure of the phenylene-bridged macrocage **1** modeled as a gyroscope-like molecule (Figure 1) [12]. It has been observed that the phenylene rotor could rotate inside the cage consisting of three silaalkane spokes, and thus, the structure of the molecule resembles that of the gyroscope, wherein the rotor spins inside a frame. Since the rotor in **1** is sterically shielded by the exterior cage, the rotor can rotate even in the densely packed crystalline state. The dynamics of the rotor was confirmed by solid-state ^{13}C CP/MAS proton dipolar dephasing (solid-state ^{13}C CP/MAS-pdp) NMR spectroscopy [16]. The CP/MAS technique is generally applied to obtain high-resolution ^{13}C-NMR spectra in the solid state. Cross-polarization (CP)

enhances the signal intensity of the carbon atoms connected to protons via energy transfer from ^{1}H to ^{13}C. Magic-angle spinning (MAS) removes the anisotropy of the chemical shift. In proton dipolar dephasing, which has been used together with the CP/MAS technique, the delay time is set after the cross-polarization in the pulse sequence. In this method, the signals of the carbon atoms that are strongly coupled with those of the proton(s) by dipole-dipole couplings are dephased, that is, weakened, depending on the delay time. Therefore, the carbon signals of the static C-H moieties are weakened, whereas the carbon signals of the dynamic C-H groups and the C atoms without proton(s) show intense peaks even at long delay time. Thus, the dynamics of the phenylene moiety of **1** could be confirmed in the crystalline state by observing the signals of the phenylene CH carbons in solid-state ^{13}C CP/MAS-pdp NMR with a long delay time. While the solid-state ^{13}C CP/MAS-pdp NMR technique is convenient to observe either the static or dynamic characteristics of the CH carbons in crystalline state, the details of the dynamics, such as the exchange model and exchange rate cannot be analyzed.

Figure 1. (**a**) Schematic representation of a gyroscope; (**b**) Structural formula of the gyroscope-like molecule **1**.

After the first report on the synthesis and solid-state ^{13}C CP/MAS-pdp study of the gyroscope-like molecule **1**, a theoretical study using DFTB calculations for the solid-state dynamics of **1** was reported [14]. According to this study, the phenylene moiety of **1** exhibited the most facile exchange among the three stationary points inside the crystal with a low activation energy (<1.2 kcal/mol). To experimentally elucidate the dynamics of the phenylene moiety, a solid-state ^{2}H NMR study of the powdered sample was planned. This spectroscopy has been widely used for the observation and analysis of the dynamics of deuterated moieties. As the natural abundance of deuterium is only 0.013%, the NMR signal(s) of deuterated moiety can be observed selectively. Moreover, the line shape and width of the spectrum, called the Pake pattern, are sensitive to the dynamics [8–11,17–20]. Herein, we report the detailed dynamics of the phenylene rotor in the gyroscope-like molecule **1** in the crystalline state by analyzing the solid-state ^{2}H NMR spectrum of **1** with a tetradeuterated phenylene rotor (**1**-d_4).

2. Materials and Methods

2.1. General Details

All the reagents and solvents were purchased from commercial suppliers and used without purifications.

2.2. Synthesis and Characterization of the Deuterated Gyroscope-Like Molecule **1**-d_4

The title compound **1**-d_4 was prepared by following the previously reported synthesis protocol of **1** [12]. The procedure has been described here briefly (Figure 2). The reaction of 1,4-dibromobenzene-d_4 with chlorotrivinylsilane in the presence of magnesium turnings in tetrahydrofuran (THF) afforded bissilylbenzene **2**-d_4. Hydrosilylation of **2**-d_4 with chlorodimethylsilane, followed by the reaction with chlorodimethylvinylsilane, produced the silylated compound **3**-d_4. This compound was then converted to the precursor **4**-d_4 by hydrosilylation and $LiAlH_4$ reduction. Hydrolysis of **4**-d_4 with aqueous KOH in a highly dilute THF solution afforded the desired compound **1**-d_4.

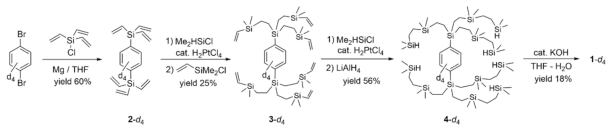

Figure 2. Synthesis of deuterated gyroscope-like molecule **1**-d_4.

Since all the intermediates and products shown in Figure 2 are new compounds, spectral data have been summarized in Appendix A and their raw data are shown in the Supplementary Materials.

2.3. Differential Scanning Calorimetry (DSC) Study

Mettler-Toledo DSC-1 equipped with a low-temperature controller was used for the DSC measurements. The data acquisition was carried out at a heating rate of 10 °C/min.

2.4. Solid-State ^2H NMR Study

Temperature-dependent solid-state ^{2}H NMR spectra were recorded on a Varian Unity 500 spectrometer, using a quadrupolar echo pulse sequence (d1-90° pulse-τ1-90° pulse-τ2-FID; 90° pulse = 4.2 μs, τ1 = 30 μs, τ2 = 20 μs, d1 = 20 s). KBr powder was used as an excipient for dilution, owing to the low amounts of the sample.

3. Results and Discussions

3.1. Outline of the Previous Report on the Dynamics of the Phenylene Moiety in **1** *in the Crystalline State*

The crystal structure of the gyroscope-like molecule **1** was found to be dependent on temperature [12]. The phenylene moiety of **1** was observed in a limited area (D, E, and F) having a deformed cage-like structure at 200 K. In contrast, at 300 K, the phenylene group was distributed in a disordered manner over three positions (A, B and C), with a symmetric cage-like structure (Figure 3) [12]. The two different structures switch at the crystal-to-crystal phase transition temperature of ~195 K. As described in the introduction, the rotation of the phenylene group at rt was confirmed by solid-state ^{13}C CP/MAS-pdp spectra of powdered **1**. Generally, the exchange rates and the mechanism of the dynamics are not discussed using this technique. While the mode of the phenylene rotation switched at the phase transition, a low temperature NMR setup was not available.

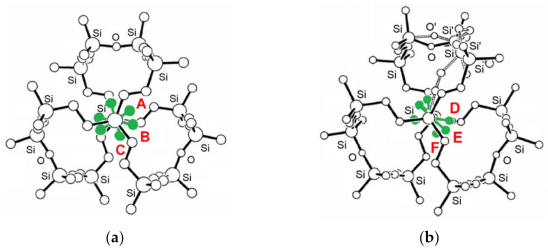

Figure 3. Structure of **1** as determined by single-crystal X-ray analysis [12] at (**a**) 303 K, Site occupancy factors: A; 0.353(9), B; 0.450(10), and C; 0.200(7); (**b**) 173 K, Site occupancy factors: D; 0.258(13), E; 0.445(14), and F; 0.293(8).

3.2. DSC Analysis of Powdered **1**

The thermodynamic parameters for the crystal-to-crystal phase transition can be confirmed from the endothermic signal in differential scanning calorimetry (DSC). Figure 4 depicts the DSC chart of powdered **1** recorded from 120 K to 400 K, of which the sample was taken from the previous study [12]. Two endothermic peaks were observed. The peak at 193.7 K is attributed to the crystal-to-crystal phase transition, whereas the peak at 385 K corresponds to the melting point, that is, the solid-to-liquid phase transition. The thermodynamic parameters, ΔH = 320 cal/mol and ΔS = 1.6 e.u., for the crystal-to-crystal transition were estimated from the observed absorption heat. According to the definition

of entropy (ΔS = R ln$W$, where R and W are the gas constant and number of degree of freedom, respectively) in statistical thermodynamics, the degree of freedom of a crystal increases by 2.2 per mole on increasing the temperature, where the numerical value is identical to the degree of freedom for 1-axis rotation (clockwise and anticlockwise rotation) of the phenylene rotor. Thus, the transition is attributed to the static-to-dynamic (rotational) phase transition.

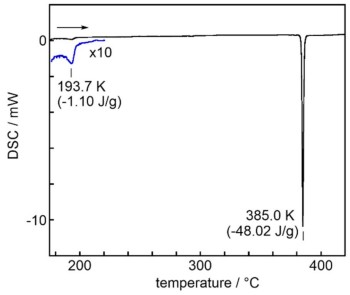

Figure 4. Differential scanning calorimetry (DSC) chart of powdered **1**.

3.3. Solid-State ^{2}H NMR Spectroscopy of Powdered **1**-d_4

Solid-state ^{2}H NMR spectroscopy is widely used to observe the molecular dynamics of deuterated moieties in the crystalline state because the line width and the shape of the spectra are sensitive to the molecular motion of the deuterated moiety [8–11,17–20]. Figure 5 shows the solid-state ^{2}H NMR spectra of powdered **1**-d_4 recorded at 300 K and 320 K. The solid lines represent the observed spectra. A signal was observed in the spectra due to quadrupole coupling. The dotted red lines represent the simulated spectra that were carried out by NMR WebLab [21]. The simulated spectra were produced by assuming fast six-site exchange (the jump angle is 60°, the rates (site p^2 to p^1, *the rate-determining step*) are 1 MHz (300 K) and 1.2 MHz (320 K), and the quadrupole coupling constant is 130 kHz.) with different populations p_n (n = 1–6, $p^1 = p^4 = 0.25$, and $p^2 = p^3 = p^5 = p^6 = 0.125$) taken from the single-crystal X-ray analysis data. Based on the above analysis, the facile rotation of the rotor was confirmed.

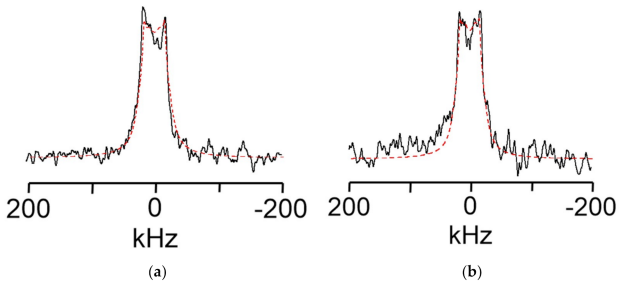

Figure 5. Solid-state ^{2}H NMR spectra of the powdered gyroscope-like molecule with a deuterated phenylene **1**-d_4 at (**a**) 300 K; (**b**) 320 K. The solid black lines and dotted red lines represent the observed and simulated spectra, respectively.

Temperature-dependent ^{2}H NMR spectra can provide useful information regarding the rotational barrier by analyzing the temperature-dependent exchange rate and their Arrhenius (and/or Eyring) plots. Thus, analysis of the spectra below 300 K is of interest. However, such an experiment could not be carried out because a long acquisition time was needed due to the lack of sample amount.

4. Conclusions

Phenylene rotation of the gyroscope-like molecule was confirmed in crystalline state by solid-state ^{2}H NMR of the powdered compound with a deuterated rotor. The NMR spectrum at 300 K indicates that the phenylene moiety exhibits facile six-site exchange with

an exchange rate of 1 MHz. This rotational mechanism and rate were in good accordance with the previously reported results of a theoretical study on the DFTB calculations for the phenylene dynamics of the compound [14]. However, more detailed information, such as energy barriers for the rotation, could not be analyzed due to limitations of the measurement. DSC analysis of the powdered samples revealed mode switching of the phenylene rotation. Analysis of the entropy change for the phase transition indicates that the switching is triggered by the crystal-to-crystal phase transition.

Supplementary Materials: The following are available online at https://www.mdpi.com/2624-8549/3/1/4/s1, Figure S1: ^{1}H NMR spectrum of deuterated gyroscope-like molecule **1**-d_4, Figure S2: ^{13}C NMR spectrum of deuterated gyroscope-like molecule **1**-d_4, Figure S3: HRMS spectrum of deuterated gyroscope-like molecule **1**-d_4, Figure S4: ^{1}H NMR spectrum of **2**-d_4, Figure S5: ^{13}C NMR spectrum of **2**-d_4, Figure S6: HRMS spectrum of **2**-d_4, Figure S7: ^{1}H NMR spectrum of **3**-d_4, Figure S8: ^{13}C NMR spectrum of **3**-d_4, Figure S9: HRMS spectrum of **3**-d_4, Figure S10: ^{1}H NMR spectrum of **4**-d_4, Figure S11: ^{13}C NMR spectrum of **4**-d_4, Figure S12: HRMS spectrum of **4**-d_4.

Author Contributions: Conceptualization, W.S. and M.K.; methodology, W.S.; formal analysis, W.S. and K.Y.; investigation, W.S.; data curation, W.S.; writing—original draft preparation, W.S.; writing—review and editing, W.S., K.Y., and M.K.; project administration, W.S.; funding acquisition, W.S. All authors have read and agreed to the published version of the manuscript.

Funding: This work was supported by a JSPS Grant-in-Aid for Scientific Research (C) (JP20K05650), the Murata Science Foundation (M20-058), Izumi Science and Technology Foundation (2018-J-88), and Iketani Science and Technology Foundation (0291033-A).

Data Availability Statement: The data presented in this study are available in the article or the supplementary materials.

Acknowledgments: The authors are grateful to Soichiro Ohmizu for the synthesis of **1**-d_4.

Conflicts of Interest: The authors declare no conflict of interest.

Appendix A

Spectroscopic data for compound **1**-d_4 and synthetic intermediates shown in Figure 2

1-d_4: colorless crystals; m.p. 105–106 °C; ^{1}H-NMR (400 MHz, $CDCl_3$, 7.24 ppm) δ −0.09 (s, 36H), 0.01 (s, 36H), 0.32–0.34 (m, 24H), 0.39–0.43 (m, 12H), 0.62–0.67 (m, 12H); ^{13}C-NMR (100 MHz, $CDCl_3$) δ −4.2, −0.5, 4.5, 5.9, 6.9, 10.2, 133.2 (t, $J_{C\text{-}D}$ = 19 Hz), 136.8; ^{29}Si NMR (79 MHz, $CDCl_3$) δ 2.1, 5.6, 8.1; HRMS (ESI) calcd for $C_{54}H_{120}D_4Si_{14}O_3Na$, 1239.6463 ([M + Na^+]); found, 1239.6463 ([M + Na^+]).

2-d_4: a colorless oil; b.p. 120 °C/3 Pa; ^{1}H-NMR (400 MHz, $CDCl_3$, δ) 5.86 (dd, J = 4.0, 20 Hz, 6H), 6.23 (dd, J = 4.0, 14 Hz, 6H), 6.35 (dd, J = 14, 20 Hz, 6H); ^{13}C-NMR (100 MHz, $CDCl_3$, δ) 133.7, 134.0 (t, $J_{C\text{-}D}$ = 12 Hz), 135.5, 136.0; ^{29}Si NMR (79 MHz, $CDCl_3$, δ) –24.1; HRMS (ESI) calcd for $C_{18}H_{18}D_4Si_2Na$,321.1403 ([M + Na^+]); found, 321.1403 ([M + Na^+]).

3-d_4: colorless crystals; mp 132–134 °C; ^{1}H-NMR (400 MHz, C_6D_6, δ) 0.06 (s, 36H), 0.60–0.64 (m, 12H), 0.89–0.94 (m, 12H), 5.68 (dd, J = 4.0, 20.0 Hz, 6H), 5.94 (dd, J = 4.0, 14.8 Hz, 6H), 6.16 (dd, J = 14.8, 20.0 Hz, 6H); ^{13}C-NMR (100 MHz, C_6D_6, δ) −3.9, 3.7, 7.8, 132.0, 133.7 (t, $J_{C\text{-}D}$ = 23 Hz), 138.1, 138.9; ^{29}Si NMR (79 MHz, C_6D_6, δ) −3.7, 3.3; HRMS (ESI) calcd for $C_{42}H_{78}D_4Si_8Na$, 837.4714 ([M + Na^+]); found, 837.4718 ([M + Na^+]).

4-d_4: colorless crystals; mp 43–44 °C; ^{1}H-NMR (400 MHz, $CDCl_3$, δ) −0.03 (s, 36H), 0.08 (d, J = 3.6Hz, 36H), 0.40–0.45 (m, 12H), 0.46–0.48 (m, 24H), 0.70–0.74 (m, 12H), 3.86 (br, 6H); ^{13}C-NMR (100 MHz, $CDCl_3$, δ) −4.8, −4.3, 3.3, 6.4, 6.7, 7.3, 133.0 (t, $J_{C\text{-}D}$ = 22 Hz), 137.8; ^{29}Si NMR (79 MHz, $CDCl_3$, δ) −10.1, 2.2, 5.8; HRMS (ESI, NaI was added as ionization agent.) calcd for $C_{54}H_{126}D_4Si_{14}I$, 1301.6243 ([M + I^-]); found, 1301.6237 ([M + I^-]).

References

1. Kottas, G.S.; Clarke, L.I.; Horinek, D.; Michl, J. Artificial Molecular Rotors. *Chem. Rev.* **2005**, *105*, 1281–1376. [CrossRef]
2. Erbas-Cakmak, S.; Leigh, D.A.; McTernan, C.T.; Nussbaumer, A.L. Artificial Molecular Machines. *Chem. Rev.* **2015**, *115*, 10081–10206. [CrossRef] [PubMed]
3. Roy, I.; Stoddart, J.F. Amphidynamic Crystals Key to Artificial Molecular Machines. *Trends Chem.* **2019**, *1*, 627–629. [CrossRef]
4. Kaleta, J.; Chen, J.; Bastien, G.; Dračínsky, M.; Mašát, M.; Rogers, C.T.; Feringa, B.L.; Michl, J. Surface inclusion of unidirectional molecular motors in hexagonal tris(o-phenylene) cyclotriphosphazene. *J. Am. Chem. Soc.* **2017**, *139*, 10486–10498. [CrossRef] [PubMed]
5. Garcia-Garibay, M.A. Crystalline molecular machines: Encoding supramolecular dynamics into molecular structure. *Proc. Natl. Acad. Sci. USA* **2005**, *102*, 10771–10776. [CrossRef]
6. Joshi, H.; Kharel, S.; Ehnbom, A.; Skopek, K.; Hess, G.D.; Fiedler, T.; Hampel, F.; Bhuvanesh, N.; Gladysz, J.A. Three-Fold Intramolecular Ring Closing Alkene Metatheses of Square Planar Complexes with cis Phosphorus Donor Ligands $P(X(CH_2)_mCH{=}CH_2)_3$ (X = −, m = 5–10; X = O, m = 3–5): Syntheses, Structures, and Thermal Properties of Macrocyclic Dibridgehead Diphosphorus Complexes. *J. Am. Chem. Soc.* **2018**, *140*, 8463–8478.
7. Commins, P.; Nuñez, J.E.; Garcia-Garibay, M.A. Synthesis of Bridged Molecular Gyroscopes with Closed Topologies: Triple One-Pot Macrocyclization. *J. Org. Chem.* **2011**, *76*, 8355–8363. [CrossRef]
8. Setaka, W.; Yamaguchi, K. Thermal modulation of birefringence observed in a crystalline molecular gyrotop. *Proc. Natl. Acad. Sci. USA* **2012**, *109*, 9271–9275. [CrossRef]
9. Setaka, W.; Yamaguchi, K. Order-Disorder Transition of Dipolar Rotor in a Crystalline Molecular Gyrotop and Its Optical Change. *J. Am. Chem. Soc.* **2013**, *135*, 14560–14563. [CrossRef]
10. Setaka, W.; Yamaguchi, K. A Molecular Balloon: Expansion of a Molecular Gyrotop Cage Due to Rotation of the Phenylene Rotor. *J. Am. Chem. Soc.* **2012**, *134*, 12458–12461. [CrossRef] [PubMed]
11. Tsurunaga, M.; Inagaki, Y.; Momma, H.; Kwon, E.; Yamaguchi, Y.; Yoza, K.; Setaka, W. Dielectric Relaxation of Powdered Molecular Gyrotops Having a Thiophene Dioxide-diyl as a Dipolar Rotor. *Org. Lett.* **2018**, *20*, 6934–6937. [CrossRef] [PubMed]
12. Setaka, W.; Ohmizu, S.; Kabuto, C.; Kira, M. A Molecular Gyroscope Having Phenylene Rotator Encased in Three-Spoke Silicon-Based Stator. *Chem. Lett.* **2007**, *36*, 1076–1077. [CrossRef]
13. Setaka, W.; Ohmizu, S.; Kira, M. Molecular Gyroscope Having a Halogen-substituted p-Phenylene Rotator and Silaalkane Chain Stators. *Chem. Lett.* **2010**, *39*, 468–469. [CrossRef]
14. Marahatta, A.B.; Kanno, M.; Hoki, K.; Setaka, W.; Irle, S.; Kono, H. Theoretical Investigation of the Structures and Dynamics of Crystalline Molecular Gyroscopes. *J. Phys. Chem. C* **2012**, *116*, 24845–24854. [CrossRef]
15. Setaka, W.; Ohmizu, S.; Kira, M. Kinetic stabilization against the oxidation reaction induced by a silaalkane cage in a thiophene-bridged molecular gyroscope. *Chem. Commun.* **2014**, *50*, 1098–1110. [CrossRef]
16. Sidhu, P.S.; Penner, G.H.; Jeffrey, K.R.; Zhao, B.; Wang, Z.L.; Goh, I. Solid-State NMR Study of Guest Molecule Dynamics in 4-Alkyl-tert-butylbenzene/Thiourea Inclusion Compounds. *J. Phys. Chem. B* **1997**, *101*, 9087–9097. [CrossRef]
17. Pake, G.E. Nuclear Resonance Absorption in Hydrated Crystals: Fine Structure of the Proton Line. *J. Chem. Phys.* **1948**, *16*, 327–336. [CrossRef]
18. Liepuoniute, I.; Jellen, M.J.; Garcia-Garibay, M.A. Correlated motion and mechanical gearing in amphidynamic crystalline molecular machines. *Chem. Sci.* **2020**, *11*, 12994–13007. [CrossRef]
19. Colin-Molina, A.; Jellen, M.J.; García-Quezada, E.; Cifuentes-Quintal, M.E.; Murillo, F.; Barroso, J.; Pérez-Estrada, S.; Toscano, R.A.; Merino, G.; Rodríguez-Molina, B. Origin of the isotropic motion in crystalline molecular rotors with carbazole stators. *Chem. Sci.* **2019**, *10*, 4422–4429. [CrossRef]
20. Hughes, A.R.; Brownbill, N.J.; Lalek, R.C.; Briggs, M.E.; Slater, A.G.; Cooper, A.I.; Frédéric, B. Ultra-Fast Molecular Rotors within Porous Organic Cages. *Chem. Eur. J.* **2017**, *23*, 17217–17221.
21. Macho, V.; Brombacher, L.; Spiess, H.W. The NMR-WEBLAB: An Internet Approach to NMR Lineshape Analysis. *Appl. Magn. Reson.* **2001**, *20*, 405–432. [CrossRef]